Experimental evidence for the dynamic Jahn-Teller effect in $La_{0.65}Ca_{0.35}MnO_3$

P. Dai
Solid State Division, Oak Ridge National Laboratory, Oak Ridge, Tennessee 37831

Jiandi Zhang
Solid State Division, Oak Ridge National Laboratory, Oak Ridge, Tennessee 37831
and Department of Physics and Astronomy, University of Nebraska, Lincoln, Nebraska 68588-0111

H. A. Mook
Solid State Division, Oak Ridge National Laboratory, Oak Ridge, Tennessee 37831

S.-H. Liou and P. A. Dowben
Department of Physics and Astronomy, University of Nebraska, Lincoln, Nebraska 68588-0111

E. W. Plummer
Solid State Division, Oak Ridge National Laboratory, Oak Ridge, Tennessee 37831
and Department of Physics, University of Tennessee, Knoxville, Tennessee 37996
(Received 7 November 1995)

Recently, it has been argued that a strong electron-phonon interaction arising from the Jahn-Teller splitting of the outer Mn *d* level plays a crucial role in understanding the nonmetal-to-metal transition observed in the $La_{1-x}A_xMnO_3$ (A=Ca,Sr,Ba) system. We show, by neutron powder diffraction, that $La_{0.65}Ca_{0.35}MnO_3$ exhibits an anomalous volume and oxygen/manganese displacement change around T_c, in qualitative agreement with the theoretical prediction. [S0163-1829(96)00830-2]

The recent rediscovery of ''colossal magnetoresistance'' (CMR) in perovskite-based $La_{1-x}A_xMnO_3$ (A = Ca,Sr,Ba)[1] has generated considerable interest in these materials. In the doping range of $0.2 \leqslant x \leqslant 0.4$, $La_{1-x}A_xMnO_3$ orders ferromagnetically and the temperature (T) dependence of the resistivity is closely related to the magnetic ordering. The ''double exchange'' model, proposed some 30 years ago,[2] has been used more recently[3] to explain the physics of the observed nonmetal-to-metal transition. However, Millis *et al.*[4] argue that double exchange alone cannot account for the large resistivity drop below the paramagnetic to ferromagnetic phase transition temperature T_c. A strong Jahn-Teller electron-phonon coupling must also play an essential role.[5,6] In particular, the polaron effect, due in part to localization of the conduction band electrons by slowly fluctuating (dynamic) local Jahn-Teller distortions, is reduced drastically below T_c, permitting the formation of a metallic state. For medium electron-phonon coupling, which is believed to be relevant to the composition range ($0.2 \leqslant x \leqslant 0.4$) where the nonmetal-to-metal transition is observed, Millis *et al.* predict that the temperature dependence of the average root-mean-square (rms) oxygen displacements is linear with a slope that is different for T above and below T_c.[5] The large elastic anharmonicity, coupled with the Jahn-Teller distortions, induces a large volume change that might have been observed.[7–10]

Although some aspects of this model such as the behavior of the resistivity[5] agree well with the existing experimental results, the central prediction of anomalous temperature dependence of the rms oxygen displacements, due directly to the electron-phonon coupling, is yet to be observed. The lack of a direct experimental proof has sparked lively debate about the relevance of the dynamic Jahn-Teller distortion in understanding the microscopic origin of the observed CMR effect.[6,11] In this paper, we present neutron diffraction data which demonstrate that the polaron effect scenario suggested by Millis *et al.* may indeed be realized in the $La_{0.65}Ca_{0.35}MnO_3$ system. Specifically, the oxygen and Mn rms displacements, obtained by neutron Rietveld analysis, are found to exhibit anomalous behavior around T_c, in qualitative agreement with the theoretical prediction.

Our neutron experiments were performed using the HB-1A triple-axis and HB-4 high-resolution powder diffractometers at the High-Flux Isotope Reactor at Oak Ridge National Laboratory. The HB-1A triple-axis spectrometer, operated in the two-axis mode with an incident beam wavelength of 2.356 Å and collimation of 40′-40′-10′-30′ in usual notation, was used for magnetization measurements. The HB-4 diffractometer has an array of 32 detectors and available instrument scattering angle between 11° and 135°. When operated using the wavelength of 1.0314 Å, it allows a maximum wavevector transfer Q ($=4\pi/\lambda \sin\theta$) of ~ 11.25 Å^{-1} to be reached.

The polycrystalline sample used in the experiments was synthesized by a solid state reaction. Starting materials La_2O_3, $CaCO_3$, and Mn were mixed in stoichiometric proportions and heated in O_2 at 1200 °C for 24 h, at 1350 °C for 50 h, and then at 1400 °C for 50 h with two intermediate grindings. The bulk magnetization, resistivity, and magnetoresistance are all consistent with previous results.[12] The fine black powder was loaded in a thin wall vanadium can which was then mounted inside a larger aluminum can filled

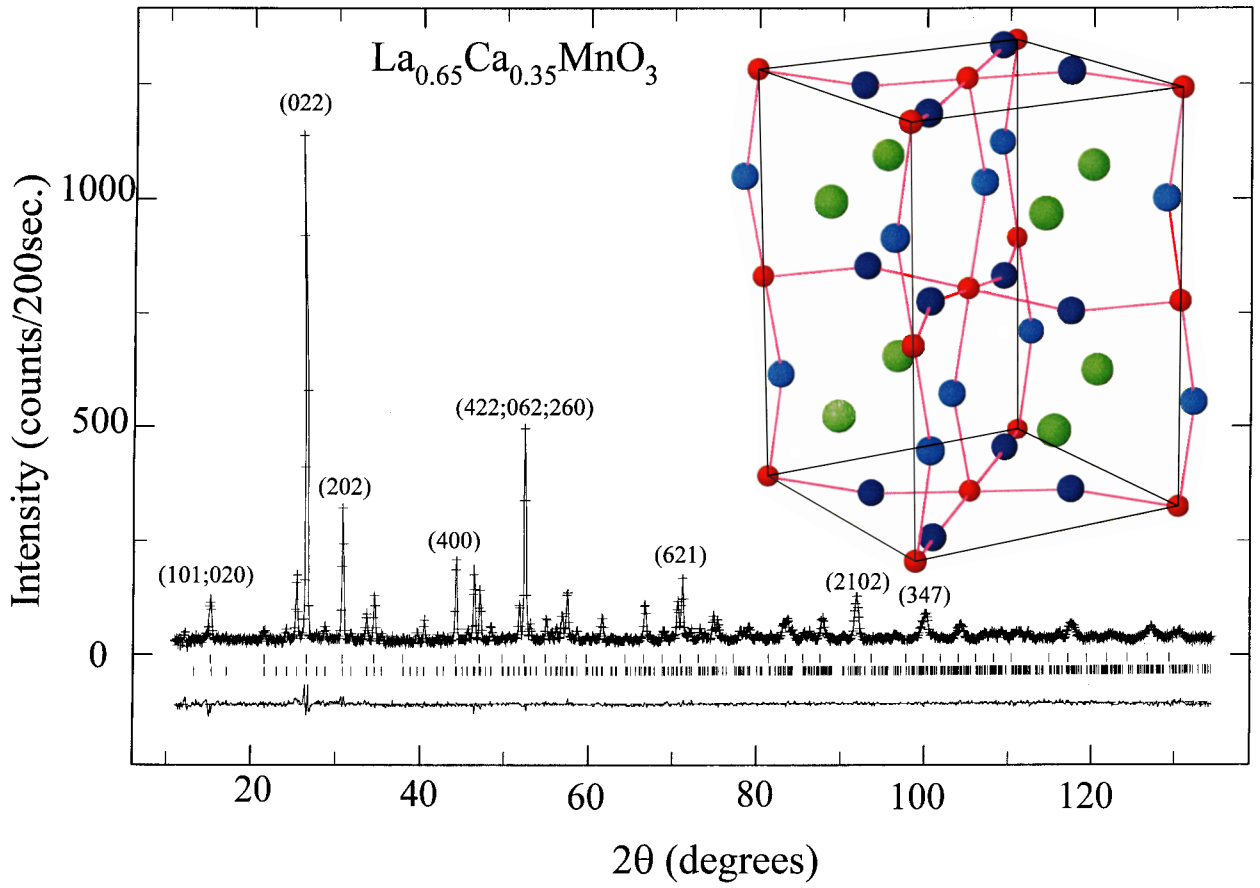

FIG. 1. Rietveld refinement patterns for $La_{0.65}Ca_{0.35}MnO_3$ at 300 K. Plus marks are observed neutron-diffraction intensities, and the solid line is calculated intensities. The first and second set of vertical marks below the profile indicate the positions of Bragg reflections for the cubic and orthorhombic structure, respectively. Major reflections are labeled with the orthorhombic indices. The curve at the bottom is the difference between the observed and calculated intensities for the orthorhombic structure. The inset shows the schematic crystal unit cell. The La/Ca, Mn, O(1), and O(2) atoms are represented in green, red, light blue, and dark blue, respectively.

with helium exchange gas. For measurements below room temperature, the aluminum can was attached to the cold finger of a Displex helium refrigerator. For higher temperature measurements, we have used an Institute Laue Langevin type furnace without the aluminum can. The temperature accuracy for the Displex is about 1 K while the high-T furnace has an uncertainty of ± 10 K.

Figure 1 shows the full pattern of the Rietveld analysis result at 300 K using the GSAS program.[13] We find that the compound has an orthorhombic structure at all the temperatures investigated with a space group *Pnma* (Ref. 14) that is different than the cubic structure proposed originally by Wollan and Koehler[7] and by Yakel[8] for this Ca composition. The conclusion of an orthorhombic unit cell is drawn, not from the the observation of line splitting, but on the basis of superlattice reflections absent in the cubic structure as shown in Fig. 1. The inset in Fig. 1 shows the unit cell structure, Table I summarizes the lattice parameters, selected bond distances, and angles obtained from the Rietveld analysis.

Having shown that the structure of our sample is orthorhombic, we now focus on the temperature dependence of the order parameter and the lattice constants. Figure 2 summarizes the results. Frame (a) displays the square of the sample magnetization, measured at zero field using the intensity change of the sum of (0,2,0) and (1,0,1) reflections as a function of temperature on warming. The 2θ angle of the reflection, directly related to the lattice parameters, is plotted in frame (b). Frames (c) and (d) show the temperature dependence of the lattice parameters and unit cell volume. The anisotropic lattice contractions around T_c are clearly evident in the data, indicating a strong coupling between the lattice and magnetism.

Although the sample structure, magnetization, and lattice parameters are important to study, such information will not

TABLE I. Refined parameters for lattice constants, selected bond distances, and angles at 300 and 40 K. Numbers in the parenthesis are statistical errors of the last significant digit. O(1)-Mn and O(2)-Mn are along the b axis and in the a-c plane, respectively.

Parameter	$T=300$ K	$T=40$ K
a (Å)	5.4537(4)	5.4371(6)
b (Å)	7.7042(6)	7.6793(7)
c (Å)	5.4682(4)	5.4496(5)
O(1)-Mn(Å)	1.9562(6)	1.9512(7)
O(2)-Mn(Å)	1.9596(26)	1.9512(24)
O(2)-Mn(Å)	1.9557(26)	1.9507(25)
Mn-O(1)-Mn(°)	159.86(19)	159.42(20)
Mn-O(2)-Mn(°)	160.99(11)	161.11(12)

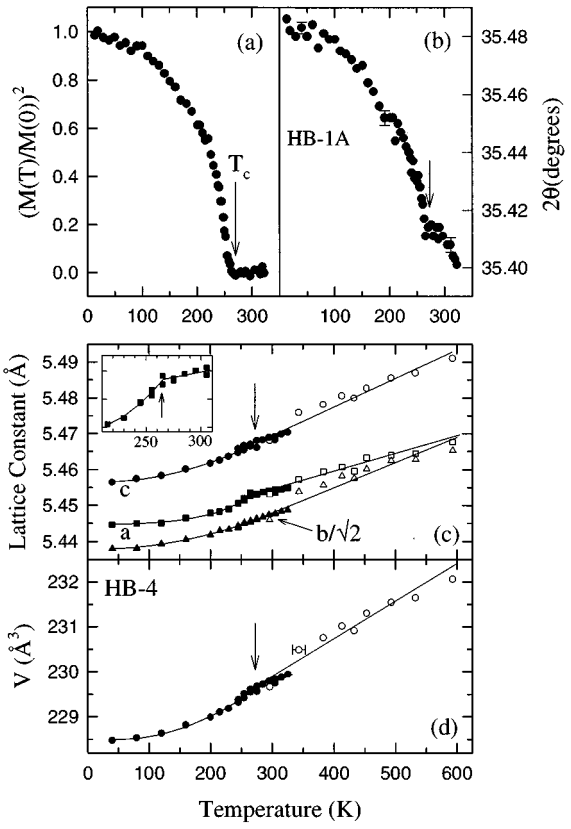

FIG. 2. (a) Reduced magnetization vs temperature on warming up (●), obtained by subtracting the background and normalizing the data to the intensity at 40 K. (b) 2θ angle vs T for (1,0,1) and (0,2,0) Bragg reflections. (c) Lattice parameters as a function of temperature. The inset shows an expanded version of the a lattice constant. (d) unit cell volume vs T. For HB-4 data, closed symbols are measurements obtained with a Displex helium refrigerator while open symbols are furnace results. The errors in the lattice parameters are less than the size of the symbol. The lattice parameter differences at room T between closed and open symbols are due mostly to systematic errors in the measurements. Solid lines are guides to the eye.

provide a direct test of the theory of the dynamic Jahn-Teller effect. Neutron diffraction, however, is also ideal for determining the oxygen rms displacements because of its sensitivity to oxygen atoms. The neutron cross section for coherent elastic scattering is proportional to e^{-2W} where the Debye-Waller temperature factor $2W(\mathbf{Q})=\langle(\mathbf{Q}\cdot\mathbf{u})^2\rangle$, and the rms displacements ($\langle\mathbf{u}^2\rangle$) are therefore mostly sensitive to the Bragg intensities at large wave-vector transfers. To test this idea, Rietveld analysis was performed for $T=300$ and 493 K data where no magnetic intensity is present in Bragg reflections. We find that all the parameters are essentially the same using a full ($11°\leqslant 2\theta\leqslant 135°$) and a partial ($60°\leqslant 2\theta\leqslant 135°$) pattern. Consequently, we have only analyzed the partial pattern for all the temperatures to avoid complication of magnetic ordering.[15]

The procedure for analyzing the temperature dependence of the HB-4 powder data is as follows. First, we simultaneously refined the scale factor, background, and peak profile, lattice parameters, atomic positions, and Debye-Waller factors for all the atoms[16] for the 40 K data set. The peak

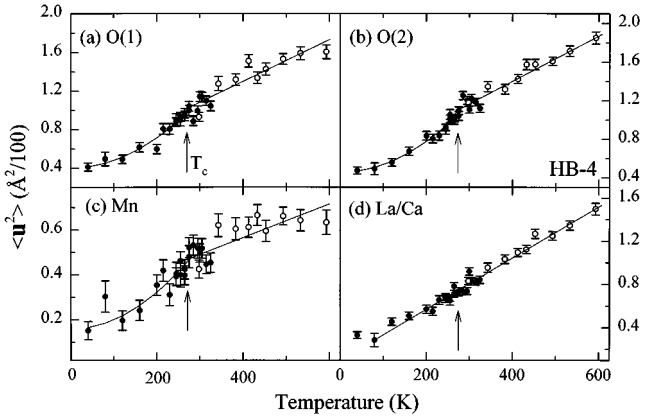

FIG. 3. Isotropic Debye-Waller factors vs T as obtained from Rietveld refinements for (a) O(1), (b) O(2), (c) Mn, and (d) La/Ca. Solid lines are guides to the eye.

profiles were then fixed to the optimum values at 40 K and other parameters allowed to vary in subsequent refinements for higher temperatures. For all the refinements, weighted R factors (R_{wp}) of ~7% were obtained with a reduced χ^2, about 1.2.

Figure 3 summarizes the outcome for the temperature dependence of the atomic rms displacements for all the atoms in the unit cell. Frames (a) and (b) show the results for oxygen at two different sites [see inset of Fig. 1]. For conventional materials such as aluminum, the atomic Debye-Waller factor W, therefore the rms displacement, is linear as a function of temperature.[17] If higher order anharmonic effects are important, W will contain additional terms which vary as T^2 and T^3. Instead of being linear, the data bear great resemblance to the T dependence of the lattice parameters. To determine whether the observed anomalous behavior in W can be entirely accounted for by the lattice expansion, we note that W, in the simplest phenomenological model, is related to volume by $W(T_2)/W(T_1)=[V(T_2)/V(T_1)]^{2\gamma}$, where γ is the Grüneisen constant, which for most materials is between 2 and 3.[17] If the observed anharmonicity in W is due entirely to volume expansion, one would expect the effective γ, or γ_{eff}, computed from W and V to be less than 3. Instead, we find that $\gamma_{\text{eff}}\simeq 85$ for T between 260 and 40 K and ~25 between 600 and 260 K, suggesting that the volume expansion is too small to account for the change in W. In the theory of the dynamic Jahn-Teller effect,[4,5] the T dependence of the rms oxygen displacements is expected to be linear with a slope that is different for temperatures above and below T_c. Our data agree with the model fairly well for T above T_c, but deviate from it at low temperatures. The presence of the nonlinear T dependence in the oxygen rms displacements suggests a strong elastic anharmonicity in the crystal below T_c. Such anharmonicity, although known to be present, is not considered explicitly in the model of Millis *et al.*[5] Therefore, calculations that include detailed structural information, and possibly quantum effects, will be required before a quantitative comparison between theory and experiment can be made.

Finally in Figs. 3(c) and (d), the rms displacements of Mn and La/Ca are plotted. It is clear that Mn exhibits a temperature dependence similar to the oxygen atoms while La/Ca

has the normal Debye-Waller factor behavior. Although the T dependence of the rms displacements for Mn and La/Ca is not predicted directly in the theory, this result is not surprising given that the bond lengths of the La/Ca-O (2.41–3.11 Å) and La/Ca-Mn (3.25–3.42 Å) atoms are much larger than that of the Mn-O (1.95 Å) atoms. Therefore, the influence of the apparent anharmonicity and dynamic Jahn-Teller distortions is greatly reduced for the La/Ca atoms.

One of the key issues in understanding the microscopic origin of the CMR in these perovskites is the possible coupling among structural, electronic, and magnetic phase transitions. Recent work by Hwang *et al.*[10] has demonstrated a direct linkage between the Curie temperature T_c and the average ionic radius of the La site $\langle r_A \rangle$ in $La_{0.7-x}B_xCa_{0.3}MnO_3$ (B = Pr, Y). Similarly, the size of the doping divalent alkaline-earth ions in $La_{1-x}A_xMnO_3$ can also significantly affect its structural and magnetic properties. During the course of this work, we have learned of a neutron scattering experiment by Martin *et al.*[18] on the $La_{0.7}Sr_{0.3}MnO_3$ metallic ferromagnet, which has a similar doping level as $La_{0.65}Ca_{0.35}MnO_3$. The authors concluded that for this Sr composition the oxygen rms displacements are independent of the temperature being above or below T_c. We note, however, that the paramagnetic to ferromagnetic phase transition in the $La_{0.7}Sr_{0.3}MnO_3$ corresponds to a metal-to-metal transition which, according to Millis *et al.*,[5] has a weaker electron-phonon coupling and hence less anomalous behavior in the oxygen Debye-Waller factors. For $La_{0.65}Ca_{0.35}MnO_3$, the smaller Ca ionic size may facilitate a stronger electron-phonon interaction, thereby inducing the localization of the conduction band electrons above T_c and causing the observed metal-to-nonmetal transition.

In conclusion, we have studied the structural and magnetic phase transitions in perovskite $La_{0.65}Ca_{0.35}MnO_3$ by neutron powder diffraction. Our results indicate that the compound has an orthorhombic structure at all temperatures investigated. An anomalous volume, oxygen, and Mn rms displacement change around T_c is discovered. These results are in qualitative agreement with the dynamic Jahn-Teller distortions theory.[4,5]

Note added. After the submission of this paper, related diffraction results on $La_{1-x}Ca_xMnO_3$ ($x=0.25,0.5$) have been published by P.G. Radaelli *et al.* [Phys. Rev. Lett. **75**, 4488 (1995)].

We are grateful to B.C. Chakoumakos, R.M. Moon, S.E. Nagler, R.M. Nicklow, and A.J. Millis for helpful discussions. This research was supported by U.S. DOE under Contract No. DE-AC05-84OR21400 with Lockheed Martin Energy Systems, Inc., at ORNL, NSF Grants No. DMR 92-21655 and No. OSR-9255225 at Univ. of Nebraska.

[1] K. Chabara *et al.*, Appl. Phys. Lett. **63**, 1990 (1993); R. von Helmolt *et al.*, Phys. Rev. Lett. **71**, 2331 (1993); S. Jin *et al.*, Science **264**, 413 (1994); Y. Tokura *et al.*, J. Phys. Soc. Jpn. **63**, 3931 (1994).

[2] C. Zener, Phys. Rev. **82**, 403 (1951); P.W. Anderson and H. Hasegawa, *ibid.* **100**, 675 (1955); P.G. DeGennes, *ibid.* **118**, 141 (1960).

[3] C.W. Searle and S.T. Wang, Can. J. Phys. **48**, 2023 (1970); K. Kubo and N. Ohata, J. Phys. Soc. Jpn. **33**, 21 (1972); N. Furukawa, *ibid.* **63**, 3214 (1994).

[4] A.J. Millis *et al.*, Phys. Rev. Lett. **74**, 5144 (1995).

[5] A. J. Millis *et al.*, Phys. Rev. Lett. (to be published).

[6] K. Bärner *et al.*, Phys. Status Solidi B **187**, K61 (1995); W.H. Jung and E. Iguchi, J. Phys. Condens. Matter **7**, 1215 (1995); M.I. Salkola *et al.*, Phys. Rev. B **51**, 8878 (1995); J. Zang *et al.*, *ibid.* **53**, R8840 (1996).

[7] E.O. Wollan and W.C. Koehler, Phys. Rev. **100**, 545 (1955).

[8] H.L. Yakel, Acta Crystallogr. **8**, 394 (1955).

[9] K. Knížek, *et al.*, J. Solid State Chem. **100**, 292 (1992).

[10] H.Y. Hwang *et al.*, Phys. Rev. Lett. **75**, 914 (1995).

[11] N. Furukawa, J. Phys. Soc. Jpn. **64**, 2734 (1995); **64**, 2754 (1995).

[12] P. Schiffer *et al.*, Phys. Rev. Lett. **75**, 3336 (1995).

[13] A.C. Larson and R.B. Von Dreele, GSAS-General Structure Analysis System (Los Alamos National Laboratory, 1986).

[14] J.B.A.A. Elemans *et al.*, J. Solid State Chem. **3**, 238 (1971).

[15] Because of the Mn magnetic form factor, magnetic contributions to the Bragg reflections for $2\theta \geqslant 60°$ ($\sin\theta/\lambda \geqslant 0.485$) are essentially negligible. To reduce the errors for the atomic Debye-Waller factors, a slightly larger data range ($40.2° \leqslant 2\theta \leqslant 135°$) was used for T above T_c.

[16] The La/Ca and oxygen content of the sample are assumed to be ideal. Previous works on similarly prepared $La_{0.67}Ba_{0.33}MnO_z$ [H.L. Ju *et al.*, Phys. Rev. B **51**, 6143 (1995)] and $La_{1-x}Ca_xMnO_3$ (Ref. 12) show the oxygen stoichiometry to be within $<1\%$ of ideal. In addition, the compounds are known to be stable below 600 K.

[17] R.M. Nicklow and R.A. Young, Phys. Rev. **152**, 591 (1966).

[18] M.C. Martin *et al.*, Phys. Rev. B **53**, 14 285 (1996).